# Temperature dependence of the electron diffusion coefficient in electrolyte-filled $TiO_2$ nanoparticle films: Evidence against multiple trapping in exponential conduction-band tails

Nikos Kopidakis,* Kurt D. Benkstein, Jao van de Lagemaat, and Arthur J. Frank†
*National Renewable Energy Laboratory, Golden, Colorado 80401-3393, USA*

Quan Yuan and Eric A. Schiff‡
*Department of Physics, Syracuse University, Syracuse, New York 13244-1130, USA*
(Received 6 July 2005; revised manuscript received 20 October 2005; published 25 January 2006)

The temperature and photoexcitation density dependences of the electron transport dynamics in electrolyte-filled mesoporous $TiO_2$ nanoparticle films were investigated by transient photocurrent measurements. The thermal activation energy of the diffusion coefficient of photogenerated electrons ranged from 0.19–0.27 eV, depending on the specific sample studied. The diffusion coefficient also depends strongly on the photoexcitation density; however, the activation energy has little, if any, dependence on the photoexcitation density. The light intensity dependence can be used to infer temperature-independent dispersion parameters in the range 0.3–0.5. These results are inconsistent with the widely used transport model that assumes multiple trapping of electrons in an exponential conduction-band tail. We can also exclude a model allowing for widening of a band tail with increased temperature. Our results suggest that structural, not energetic, disorder limits electron transport in mesoporous $TiO_2$. The analogy between this material and others in which charge transport is limited by structural disorder is discussed.

DOI: 10.1103/PhysRevB.73.045326 PACS number(s): 73.63.Bd, 73.50.Pz, 73.50.Gr, 72.80.Ng

## I. INTRODUCTION

Porous semiconductors can have remarkable properties. Perhaps the best known recent example is porous silicon, which luminesces strongly when homogeneous crystalline silicon does not.[1,2] For some porous silicon structures prepared by electrochemical etching of a single crystal, the length scales of the porosity include nanometer-scale elements that apparently confine electrons and holes long enough to permit luminescence at wavelengths consistent with quantum size effects. The material also has a backbone of larger elements that permits macroscopic electrical transport. A second remarkable example of a porous semiconductor is porous titania, which is the basis of an efficient, dye-sensitized solar cell.[3,4] In this material, a mesoporous $TiO_2$ film is prepared by sintering of titania particles with a typical diameter around 20 nm. The pores are then filled with an electrolyte or a conductive polymer. The resulting, bicontinuous porous material separates the transport pathways of electrons from their countercharges (ions or holes). This separation is valuable for solar cell applications since it inhibits the recombination of photogenerated electrons with the countercharges.

These two classes of porous semiconductors are based on crystalline materials. However, for both classes, the porosity is associated with significant disorder that, for example, greatly reduces charge carrier mobilities or diffusion coefficients from the values in the underlying crystals.[5–7] This type of disorder is an interesting if little explored aspect of the enormous subject of transport in highly disordered, nominally homogeneous systems. Research on electronic properties of porous materials includes theoretical work on quantum percolation,[8–10] which applies when porosity has an atomic length scale, and studies of Coulomb-blockaded semiclassical transport on porous lattices that reveals analogies with phase transitions.[11–13]

In the present paper, we study the diffusion of photogenerated electrons in mesoporous titania. The electrolyte, which fills the pores, is not only essential to the application of this material in solar cells, but also appears to passivate defects that greatly retard electron transport in "dry" mesoporous titania.[14] Technically, diffusion of electrons in the electrolyte-filled material is ambipolar,[6,15] meaning that the mobile electrons in titania carry a cloud of countercharges (cations) in the electrolyte. This is a well-known phenomenon in the diffusion theory of electrolyte solutions.[16] Because the electron density in $TiO_2$ at typical illumination intensities (e.g., one sunlight intensity) is more than two orders of magnitude lower than the density of mobile ions in the electrolyte, the ambipolar diffusion coefficient and the electron diffusion coefficient are essentially equal.[6,17,18]

The largest group of experiments on electron diffusion involves measurements of transient photocurrents in the solar cell configuration, which incorporates a bottom, electron-collecting electrode and a top, countercharge-collecting electrode in contact with the electrolyte. There are two principal features revealed by these measurements. First, electron diffusion is Gaussian in its dependence on time and distance, which simply means that these measurements can be described adequately using a conventional diffusion coefficient $D$.[6,19,20] Second, the electron diffusion is quite nonlinear in the electron density $N$, increasing with $N$ as expressed by the power law $D(N) \propto N^{\beta}$.[6,15,21–24] Also, the diffusion coefficient depends both on the details of the preparation of mesoporous titania and on subsequent sample treatments.[7,25]

As has been noted in many of the earlier papers,[6,15,21,26–29] these aspects of the diffusion measurements over the range of light intensities or open-circuit photovoltages investigated are consistent with an "exponential conduction-band tail multiple-trapping" model; the properties of this model are well-known owing to its extensive application to amorphous

 

silicon.[30,31] The exponential conduction-band tail (CBT) model assumes the existence of a "transport edge" $E_C$ within the electronic density of states $g(E)$ of the conduction band. Electrons occupying states above the transport edge are assumed to have a well-defined electron diffusion coefficient $D_0$; this edge plays the same role in the multiple-trapping model as does the ordinary conduction-band edge in a homogeneous crystalline material. Electrons occupying the "traps" below $E_C$ are assumed to be localized, and the distribution of trap energies over the region spanned by the quasi-Fermi level is assumed to be exponential[15] $g(E) = g_C \exp[(E-E_C)/m_C]$, where $m_C$ is the slope or characteristic energy of the distribution. Such an exponential distribution is a plausible consequence of disorder.[32]

This multiple-trapping model predicts non-Gaussian (or dispersive) diffusion in the limit of low trap occupancy.[30] In the case of Gaussian diffusion, the mean square displacement of a diffusing carrier obeys $\langle x^2 \rangle \propto t$, whereas for dispersive transport the corresponding relation is $\langle x^2 \rangle \propto t^\alpha$, where $\alpha$ is the "dispersion parameter." For electrolyte-filled mesoporous titania, optically detected photocarrier recombination has been used to infer a dispersion parameter $\alpha = 0.37$.[24] For band tail multiple trapping, $\alpha = k_B T/m_C$ (where $k_B$ is Boltzmann's constant and $T$ is the temperature), which for the reported value of $\alpha$ yields $m_C = 68$ meV.

As noted above, dispersion is not directly evident in photocurrent transient measurements. However, the measured Gaussian diffusion and photocharge density-dependent diffusion have been successfully explained by incorporating trap filling within multiple trapping; for a multiple-trapping model, the dispersion parameter is related to the density-dependence exponent $\beta$ by $\alpha = 1/(1+\beta)$. Typical values of $\beta$ range between 1 and 2,[6,15,33] corresponding to dispersion parameters 0.3–0.5 and conduction-band tail widths 50–80 meV.

Notwithstanding these successes, the evidence for an exponential-band tail in electrolyte-filled mesoporous titania is not conclusive. There have been no optical absorbance measurements that indicate an exponential-band tail of the same width suggested by these transport experiments. Single-crystal anatase $TiO_2$ exhibits an Urbach (exponential) absorbance tail with a temperature dependence that is consistent with excitonic effects.[34] These measurements can be used to infer that the width of the exponential-band tails (in single-crystal anatase) is much less than the 50–80 meV values inferred from diffusion measurements in the much more disordered, mesoporous material. Urbach tails cannot be readily measured in dye-sensitized cells. In nonsensitized, air-filled materials, an Urbach tail width of 78 meV at room temperature is reported.[22] It is not clear how this tail width is distributed between excitonic effects and band tails, and it would be quite interesting, indeed, in the context of the present work, to measure the temperature-dependent Urbach tails in such materials.

The exponential-band tail model implies a strong temperature dependence of diffusion. The model also predicts that the activation energy of the electron diffusion coefficient should depend strongly on the photoinduced charge density as discussed below. However, there have been no direct measurements to test either prediction. The combination of spectral and temperature-dependent measurements were central to the acceptance of the exponential-band tail picture for amorphous semiconductors.[30,35]

In the present paper, we present such temperature-dependence measurements of the electron diffusion coefficient in several samples of electrolyte-filled mesoporous titania. These measurements are summarized by the phenomenological expression

$$D(T,N) = D_0 (N/N_C)^\beta \exp(-E_{act}/k_B T), \tag{1}$$

where $\beta$, $N_C$, and $E_{act}$ are fitting parameters. This expression is shown to be inconsistent with the temperature dependence for $D(T,N)$ predicted by the exponential-band tail multiple-trapping model in two respects: (a) the activation energy $E_{act}$ does not depend on the electron density, contrary to the predicted logarithmic dependence of $E_{act}$ on $N$, and (b) the dispersion parameter $\alpha$ calculated from $\beta$ has negligible temperature dependence, instead of the proportionality to temperature predicted by the exponential-band tail model.

This negative result–that the exponential-band tail model is inconsistent with temperature-dependent electron diffusion measurements in mesoporous titania–is the most significant conclusion of the present work. We have also ruled out the extension of this model that allows for a temperature-dependent or energy-dependent band tail width $m_C$. Electron diffusion in mesoporous titania is thus qualitatively similar to nanoporous silicon, which is certainly the best-studied porous semiconductor. Samples of porous silicon also exhibit dispersive transport for both electrons and holes, and the measured temperature dependence is again too weak to be consistent with band tail multiple trapping.[5] Temperature-independent dispersion is actually fairly common in polymeric and organic semiconductors.[36,37]

We do not presently have a theory to explain the features of electrical transport in these porous materials. The early work on dispersion by Scher and Montroll[38] envisioned weakly temperature-dependent transport as one possibility for a continuous-time random walk (CTRW). Historically, the observation of temperature-independent dispersion has typically led to the conclusion that transport is dominated by "structural" as opposed to energetic disorder. An elementary model of energetic disorder is band-tail trapping. We are unaware of a comparably elementary model for predominantly structural disorder.

## II. EXPERIMENTAL METHODS

Mesoporous $TiO_2$ films were prepared as detailed elsewhere.[15] A thin compact $TiO_2$ buffer layer was deposited on the conducting glass (TCO; $F:SnO_2$; 8 $\Omega$/sq) prior to depositing the $TiO_2$ nanoparticle film. The resulting annealed films were about 7 $\mu$m thick with a porosity of about 60%.

Cells with nonsensitized and sensitized $TiO_2$ films were prepared for charge transport measurements. The nonsensitized cells also contained a Pt foil counter electrode and an

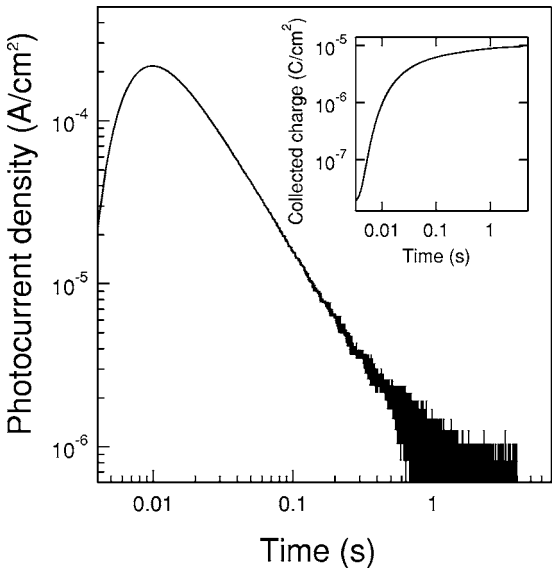


FIG. 1. Photocurrent transient for a nonsensitized $TiO_2$ nanoparticle film in 0.1 M $TBAClO_4$/ethanol, induced by 337 nm laser pulses. The inset shows the collected charge determined from the time integral of the photocurrent.

Ag/AgCl wire reference electrode. These cells were filled with 0.1 M tetrabutylammonium perchlorate ($TBAClO_4$) in ethanol. The edges of the working electrodes were covered with TorrSeal resin to prevent contact of the conducting glass substrate with the electrolyte. Excitation of photocarriers in nonsensitized $TiO_2$ occurred by UV laser pulses (337 nm, 3 ns duration) from a nitrogen laser incident on the outermost surface of the film. The temperature of the cell was thermostatically controlled between 263 and 318 K. Potential control was obtained using an EG&G model 283 potentiostat, and transients were recorded with a digital oscilloscope. All transient photocurrent measurements were performed at 0 V vs Ag/AgCl.

Dye-sensitized $TiO_2$ solar cells were prepared as detailed elsewhere.[6] The cells were filled with a high-boiling point (119 °C) electrolyte (0.8 M 1,2-dimethyl-3-hexylimidazolium iodide and 50 mM $I_2$ in methoxyacetonitrile). The sensitized $TiO_2$ cell was probed with 670 nm laser pulses (3 ns duration) from a nitrogen-pumped dye laser. The 670 nm light is only weakly absorbed by the dye and, therefore, provides a relatively uniform photocarrier density across the $TiO_2$ film. Transient photocurrents were measured at short circuit with a digital oscilloscope through a current preamplifier. The cells were mounted on a cryostat for temperature control. In both sample arrangements, the laser pulse intensity was varied using neutral density filters.

## III. RESULTS

Figure 1 shows a typical photocurrent transient of the nonsensitized $TiO_2$ film produced by a 337 nm laser pulse. Because anatase $TiO_2$ (3.2 eV band gap) absorbs strongly at 337 nm, electron-hole pairs are generated in a narrow ($<1$ $\mu$m) spatial region near the outermost surface of the $TiO_2$ nanoparticle layer. Some photogenerated electron-hole pairs will recombine, while others escape recombination because of the hole reaction with the solvent, a process occurring in the nanosecond regime.[39] The surviving electrons in the $TiO_2$ film diffuse through the nanoparticle network to the conducting glass substrate where they are collected. Because electron diffusion is ambipolar, the current is detected when electrons reach the collecting substrate.[6] The peak of the photocurrent transient signifies the arrival of the leading edge of the electron distribution at the collector.[6,15,18] The inset of Fig. 1 shows the collected charge. A diffusion time for electrons is estimated from the time $\tau$ when half of the electrons have arrived at the collector—i.e., the time when the collected charge is half of its saturation value.[5,6] The same method is used to obtain the diffusion time in dye-sensitized $TiO_2$ films, where the photocurrent traces are induced by uniformly absorbed 670 nm laser pulses.[6]

The electron diffusion coefficient can be calculated using $D=L^2/\tau$,[6,15] where $L$ is either the film thickness $d$ (for near surface absorption in the nonsensitized films) or $d/2$ (for uniform absorption in the sensitized films). The average photocharge density $N$ is given by $N=Q_0/(Adq_e)$, where $Q_0$ is the charge at saturation, where all of the electrons are collected, $A$ is the projected sample area, and $q_e$ is the elementary charge.

Figure 2 shows the electron diffusion coefficient as a function of $N$ between $10^{16}$ and $5\times10^{17}$ $cm^{-3}$. At the highest average photoelectron densities ($>10^{17}$ $cm^{-3}$), the electron diffusion coefficient of nonsensitized $TiO_2$ nanoparticle films becomes constant and depends on the potential applied at the $TiO_2$ electrode (i.e., the conducting $F:SnO_2$ substrate). This effect was not observed for sensitized films at comparable average photoexcitation densities when uniform photoexcitation was used. In the region of average photoexcitation densities below $10^{17}$ $cm^{-3}$, the electron diffusion coefficient in nonsensitized films does not depend on the potential applied to the substrate, which indicates that it corresponds to electrons in the electric-field-free $TiO_2$ nanoparticle film.

An important aspect of the diffusion coefficient is its power-law dependence on the photoexcitation density: $D\propto N^{\beta}$. This dependence was observed at all photoexcitation densities for sensitized films (uniform photoexcitation) and at average photoexcitation densities below $10^{17}$ $cm^{-3}$ for nonsensitized films.

Figure 3 shows the temperature dependence of the diffusion coefficient for three samples at different photoexcitation densities. The lines through the measurements represent fits to a phenomenological model for $D(T,N)$ [see Eq. (1)]. We discuss the fitting parameters below, following a comparison of the data with the conduction-band tail model.

There have been few temperature-dependent measurements on mesoporous $TiO_2$ with which to compare these data. Measurements of the temperature dependence of the saturation current in $Pt/TiO_2$ Schottky barrier structures yields a barrier height of 1.7 eV in porous nanoparticle $TiO_2$ films at high temperatures, where conduction is predominantly intrinsic.[22] Impedance spectroscopy measurements of mesoporous rutile and anatase, gas-filled $TiO_2$ nanoparticle electrodes yield an activation energy for electrical conductiv-

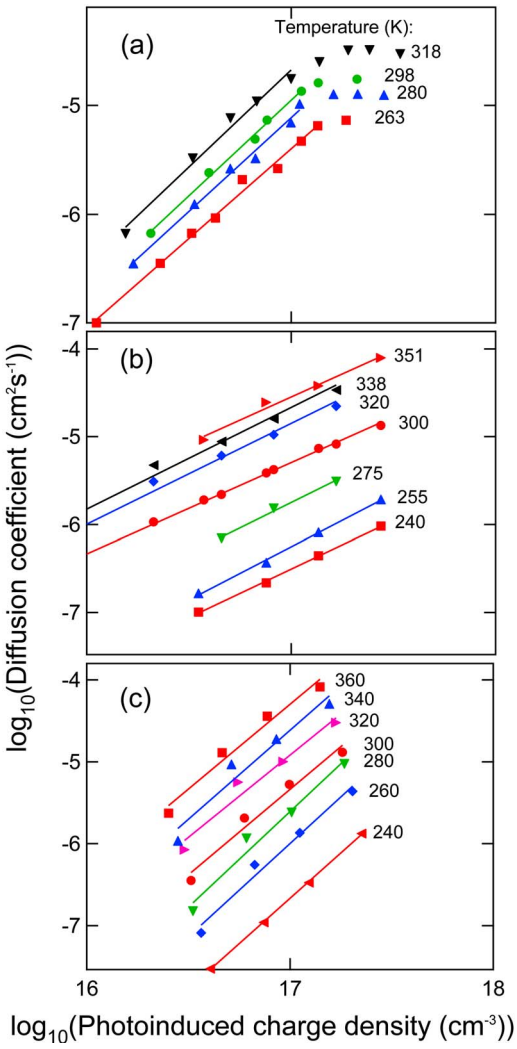


FIG. 2. (Color online) Dependence of the electron diffusion coefficient on the collected charge density for three $TiO_2$ nanoparticle films at different temperatures: (a) nonsensitized film (sample *A* of Table I) and (b) and (c) sensitized films (samples *B* and *C* of Table I). Lines are power-law fits to the data.

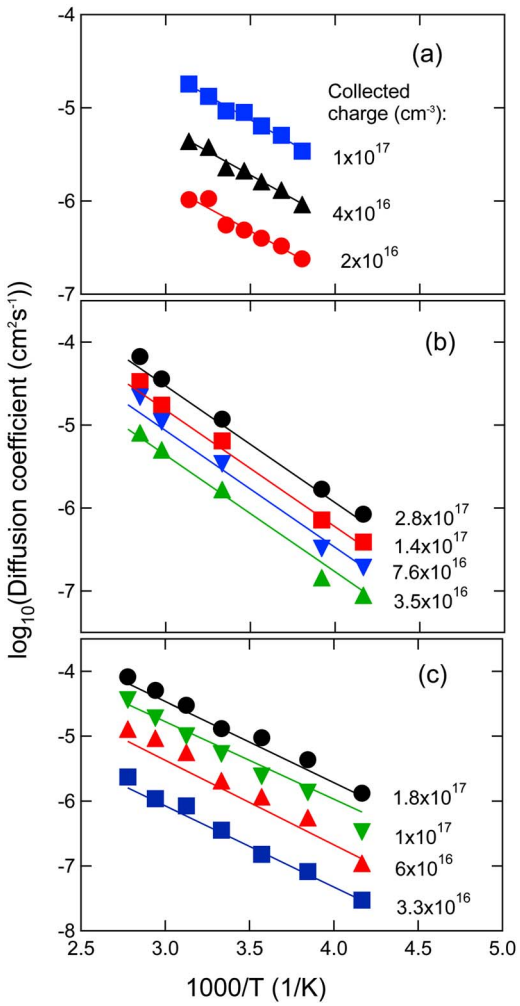


FIG. 3. (Color online) Dependence of the electron diffusion coefficient on reciprocal temperature for samples of Fig. 2: (a) nonsensitized film (sample *A* of Table I), and (b) and (c) sensitized films (samples *B* and *C* of Table I). Lines represent fits to data corresponding to $D(T,N)$ [Eq. (1)].

ity of about 0.85 eV, irrespective of the crystal structure of the material, particle size, and oxygen pressure.[40] A similar result was obtained from time-of-flight experiments, which gave an activation energy of 0.75–0.8 eV for drift mobility and 0.8–0.9 eV for electrical conductivity.[41] Previously, the same group reported an activation energy of 0.45 eV for electron mobility in porous $TiO_2$ films.[42] None of these studies considers the effect of electron density or an electrolyte on the activation energy or measures the electron mobility or diffusion coefficient directly. In a recent work, the temperature dependence of the electron mobility in electrolyte-filled $TiO_2$ matrices was inferred by combining conductivity and charge accumulation measurements.[43] For a low number of electrons per particle, the deduced activation energy of the electron mobility was 0.3 eV independent of the potential applied to the $TiO_2$ electrode, in good agreement with our results.

## IV. COMPARISON WITH MULTIPLE TRAPPING IN AN EXPONENTIAL-BAND TAIL MODEL

Within the framework of the exponential CBT model, the power-law dependence of $D$ on $N$ is attributed to trap filling. For a band tail with characteristic energy $m_C$, which corresponds to the average trap depth, the dependence of the diffusion coefficient on photoinduced charge density is given by the relation[6,15]

$$D \propto N^{(1-\alpha)/\alpha}, \tag{2}$$

where the dispersion parameter $\alpha$ is given by[6,15]

$$\alpha = \frac{k_B T}{m_C}. \tag{3}$$

The values for $\alpha$ at room temperature are typically in the range of 0.3–0.5, corresponding to $m_C$ values ranging from 60–100 meV.[6,15] Equation (2) was derived originally to ac-

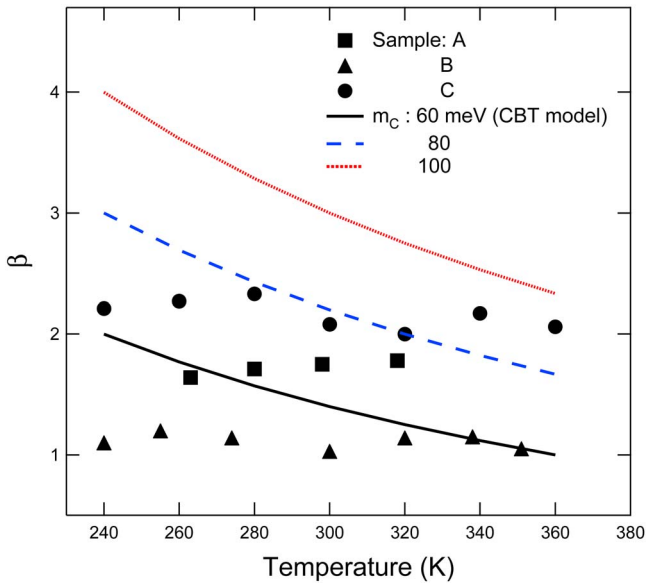


FIG. 4. (Color online) Dependence of the slope $\beta$ of power-law fits [Fig. 2; Eq. (1)] on temperature. Symbols in parentheses correspond to samples in Fig. 2(a) (squares), Fig. 2(b) (triangles), and Fig. 2(c) (dots). Lines represent the prediction of the static exponential conduction-band tail model [Eqs. (3) and (4)] with different values of the band-tail parameter $m_C$.

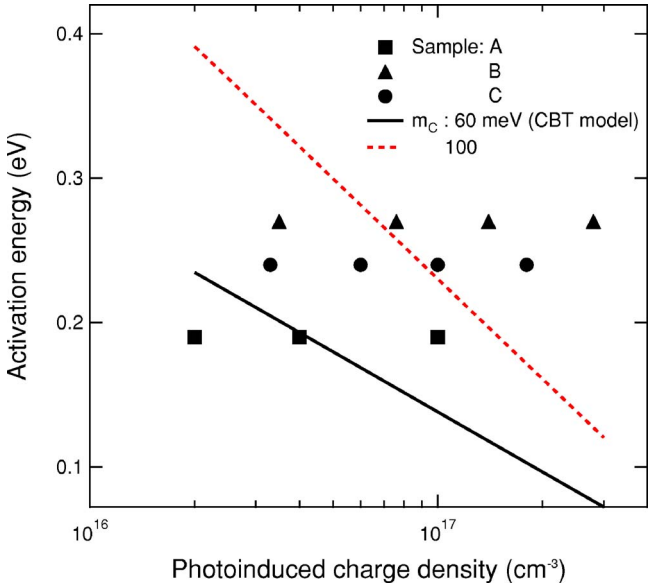


FIG. 5. (Color online) Activation energy of the electron diffusion coefficient as a function of photoinduced electron density determined from data in Fig. 3. Symbols in parentheses correspond to samples in Fig. 3(a) (squares), Fig. 3(b) (triangles), Fig. 3(c) (dots). Lines represent the prediction of the static exponential conduction-band tail model with different values of the band-tail parameter $m_C$ at a total trap density of $10^{18}$ cm$^{-3}$.

count for transient photocurrent measurements of sensitized nanoparticle films, but it also applies to nonsensitized $TiO_2$ films.[25]

Combining Eqs. (1) and (2) yields the relation between the nonlinearity of diffusion and the underlying dispersion

$$\beta = \frac{1-\alpha}{\alpha}. \tag{4}$$

It follows, therefore, that in this model $\beta$ should depend on temperature [Eq. (3)]. Contrary to this prediction, the data in Fig. 2 shows that $\beta$ does not depend on temperature. Figure 4 shows the temperature dependence of $\beta$, which is determined from the power-law fits in Fig. 2, along with the predictions of the exponential CBT model [Eqs. (3) and (4)] for $m_C$ values of 60, 80, and 100 meV. Similar results were obtained for other $TiO_2$ films investigated (not shown). In each case, the slope $\beta$ of the $D$ vs $N$ power-law plot did not depend significantly on the temperature.

Figure 5 displays the activation energy of the electron diffusion coefficient for average photocharge densities between $2\times10^{16}$ and $3\times10^{17}$ cm$^{-3}$; the data are from the fits in Fig. 3. Activation energies of the electron diffusion coefficient in different samples ranged from 0.19–0.27 eV. In each sample, the activation energy was independent of the photoelectron density.

From the exponential CBT model, it is straightforward to show that the activation energy for electron transport $E_{act}$ is determined by traps in the vicinity of the quasi-Fermi level. Therefore, it follows that $E_{act}$ should depend on the photoinduced electron density.[15]

$$E_{act} = -m_C \ln\frac{N}{g_{tot}}, \tag{5}$$

where $g_{tot}$ is the total density of states in the CBT. Equation (5) indicates that the activation energy should decrease with increasing charge. Figure 5 shows the predicted activation energy using Eq. (5). For a $m_C$ of 60 meV, the static CBT model predicts the activation energy to decrease by 0.15 eV when the photocharge density increases from $2\times10^{16}$–$3\times10^{17}$ cm$^{-3}$. Figure 5 shows that this predicted change is not observed.

Inasmuch as the static CBT model cannot explain the observed results, one might consider a CBT that widens with temperature in such a way that the band-tail parameter $m_C$ varies linearly with temperature. This would result in $\alpha$ [Eq. (3)] being independent of temperature. The band-tail parameter of polysilicon[44] and other semiconductor materials with a large density of grain boundaries is predicted and observed to increase with temperature owing to the temperature dependence of the Debye length inside the grains.[45] The latter effect cannot occur in the present system because the Debye length inside the grains is already much larger than the 20 nm grain diameter. Furthermore, from a straightforward analysis of the temperature dependence of the electron diffusion coefficient for a temperature-dependent band-tail parameter, one would expect that $D$ would *decrease* with increasing temperature, contrary to observations. One might also consider a CBT model that is not strictly exponential.[46] However, one would expect that if trap emission were a thermally activated single or multiphonon process, the activation energy of the diffusion coefficient would still depend on the

TABLE I. Fitting parameters for diffusion coefficient $D(T,N)$ [Eq. (1)].[a]

| Sample | $N_C(\mathrm{cm}^{-3})$ | $\beta$ | $E_{\mathrm{act}}$ |
|---|---|---|---|
| *A* (nonsensitized) | $2.2\times10^{17}$ | 1.7 | 0.19 |
| *B* (sensitized) | $2.0\times10^{17}$ | 1.0 | 0.27 |
| *C* (sensitized) | $2.0\times10^{17}$ | 2.2 | 0.24 |

[a]$D_0$ value of 0.275 $\mathrm{cm}^2/\mathrm{s}$ is used based on Hall mobility measurements of single-crystal anatase $TiO_2$ (see Ref. 47).

electron density in the absence of quasi-Fermi level pinning. Furthermore, even if the quasi-Fermi level were pinned by a large trap density, which would result in an electron-density independent $E_{\mathrm{act}}$, this variation of the CBT model would not explain the observed dependence of the electron diffusion coefficient on the electron density.

## V. DISCUSSION

While our experimental results do not have the form expected from an exponential-band tail, they do have a fairly simple phenomenological form in which the dependencies on photoexcitation density and on temperature are separable [Eq. (1)].

For convenience, we assume that the diffusion coefficient $D_0$ is 0.275 $\mathrm{cm}^2/\mathrm{s}$, which is the value estimated for single crystal anatase $TiO_2$.[47] We summarize the resulting estimates of $N_C$, $\beta$, and $E_{\mathrm{act}}$ in Table I. The variation of the values of $\beta$ for the three samples (from 1–2.2) is substantial. Even larger variations were found in previous experiments on individual samples when Li was intercalated into $TiO_2$ matrices.[25] The activation energy $E_{\mathrm{act}}$ also varies between samples, ranging from 0.19–0.27 eV. Interestingly, the value for $N_C$ changes relatively little for the three samples studied here. $N_C$ is also roughly comparable to the number density of anatase nanocrystallites in mesoporous films. The normalization of the photoinduced electron density with the density of $TiO_2$ nanoparticles is consistent with the proposal that localization of electrons is a phenomenon that seems to involve the entire particle.[48]

Besides the models discussed above, we have also considered variable-range hopping involving both exponential and Gaussian densities of states, and neither can explain the present results. An important conclusion of this study is that the exponential-band tail model cannot explain the experimental results and, therefore, that a different explanation for electron transport in $TiO_2$ is required. It seems likely that the assumption of a transport edge that is implicit in multiple-trapping models fails for mesoporous titania.

Mesoporous titania, at least when electrolyte-filled, appears to belong to a class of materials that exhibit dispersive transport without the strong temperature dependence of the exponential-band tail model. Porous silicon and a number of polymeric and organic semiconductors are other examples of such materials.[36,37] Such materials are typically characterized as having dispersion resulting from "structural" as opposed to "energetic" disorder with the implication that the fundamental CTRW description of traps and of a broad distribution of wait times still apply. One important distinction of the present measurements is the rapid increase of diffusion with increasing electron density. This aspect strongly suggests some type of "trap-filling" model in which traps with very long "wait times" are fairly easily removed from the waiting-time distribution (WTD).

At least one example of the relation between the structure of a nanoparticle network and dispersive transport has been demonstrated. Random walk simulations of electron transport in networks of different porosities have shown that when the porosity increases toward the percolation threshold, dispersive transport extends to much longer time scales.[7] It is also known from CTRW simulations, that an *exclusive* random walk with a WTD having the form $\phi(t)\propto t^{-1-a}$, which is independent of the assumption of energetic disorder, will indeed lead to the observed charge dependence of $D$ with a parameter $\beta$ described by Eq. (4).[19] It is not known whether the fractal disorder of the titania film combined with trapping will lead to WTDs of the same form. It would be interesting to have more theoretical and experimental tests of this speculation.

## ACKNOWLEDGMENTS

This work was supported by the Office of Science, Division of Chemical Sciences, and the Office of Utility Technologies, Division of Photovoltaics, U.S. Department of Energy, under Contract No. DE-AC36-99GO10337.

*Electronic address: nikos_kopidakis@nrel.gov
†Electronic address: afrank@nrel.gov
‡Electronic address: easchiff@syr.edu

[1] L. T. Canham, Appl. Phys. Lett. **57**, 1046 (1990).
[2] D. J. Lockwood, *Light Emission in Silicon: From Physics to Devices*, edited by D. J. Lockwood, Semiconductors and Semimetals Vol. 49 (Academic Press, New York, 1998), p. 206.
[3] B. O'Regan and M. Grätzel, Nature **353**, 737 (1991).
[4] M. Grätzel, J. Photochem. Photobiol., A **164**, 3 (2004).
[5] P. N. Rao, E. A. Schiff, L. Tsybeskov, and P. M. Fauchet, Chem. Phys. **284**, 129 (2002).
[6] N. Kopidakis, E. A. Schiff, N-G. Park, J. van de Lagemaat, and A. J. Frank, J. Phys. Chem. B **104**, 3930 (2000).
[7] K. D. Benkstein, N. Kopidakis, J. van de Lagemaat, and A. J. Frank, J. Phys. Chem. B **107**, 7759 (2003).
[8] C. Soukoulis, Q. Li, and G. S. Grest, Phys. Rev. B **45**, 7724 (1992).
[9] A. Aharony, O. Entin-Wohlman, and A. B. Harris, Physica A **200**, 171 (1993).
[10] R. Berkovits and Y. Avishai, Phys. Rev. B **53**, R16125 (1996).
[11] A. A. Middleton and N. S. Wingreen, Phys. Rev. Lett. **71**, 3198 (1993).

[12] C. P. Collier, T. Vossmeyer, and J. R. Heath, Annu. Rev. Phys. Chem. **49**, 371 (1998).
[13] S. Sachdev, K. Sengupta, and S. M. Girvin, Phys. Rev. B **66**, 075128 (2002).
[14] R. Könenkamp, P. Hoyer, and A. Wahl, J. Appl. Phys. **79**, 7029 (1996).
[15] J. van de Lagemaat and A. J. Frank, J. Phys. Chem. B **105**, 11194 (2001).
[16] L. Onsager and R. M. Fuoss, J. Phys. Chem. **36**, 2689 (1932).
[17] D. Nistér, K. Keis, S-E. Lindquist, and A. Hagfeldt, Sol. Energy Mater. Sol. Cells **73**, 411 (2002).
[18] S. Nakade, S. Kambe, T. Kitamura, Y. Wada, and S. Yanagida, J. Phys. Chem. B **105**, 9150 (2001).
[19] J. van de Lagemaat, N. Kopidakis, N. R. Neale, and A. J. Frank, Phys. Rev. B **71**, 035304 (2005).
[20] N-G. Park, J. van de Lagemaat, and A. J. Frank, J. Phys. Chem. B **104**, 8989 (2000).
[21] A. Kambili, A. B. Walker, F. L. Qiu, A. C. Fisher, A. D. Savin, and L. M. Peter, Physica E (Amsterdam) **14**, 203 (2002).
[22] R. Könenkamp, Phys. Rev. B **61**, 11057 (2000).
[23] J. van de Lagemaat and A. J. Frank, J. Phys. Chem. B **104**, 4292 (2000).
[24] J. Nelson, Phys. Rev. B **59**, 15374 (1999).
[25] N. Kopidakis, K. D. Benkstein, J. van de Lagemaat, and A. J. Frank, J. Phys. Chem. B **107**, 11307 (2003).
[26] G. Schlichthörl, S. Y. Huang, J. Sprague, and A. J. Frank, J. Phys. Chem. B **101**, 8141 (1997).
[27] J. Nelson, S. A. Haque, D. R. Klug, and J. R. Durrant, Phys. Rev. B **63**, 205321 (2001).
[28] P. E. de Jongh and D. Vanmaekelbergh, Phys. Rev. Lett. **77**, 3427 (1996).
[29] J. Bisquert and A. Zaban, Appl. Phys. A **77**, 507 (2003).
[30] T. Tiedje, in *Hydrogenated Amorphous Silicon II*, edited by J. D. Joannopoulos and G. Lukovsky (Springer, New York, 1984), p. 261.
[31] E. A. Schiff, J. Phys.: Condens. Matter **16**, S5265 (2004).
[32] C. H. Grein and S. John, Phys. Rev. B **39**, 1140 (1989).
[33] L. Dloczik, O. Ileperuma, I. Lauermann, L. M. Peter, E. A. Ponomarev, G. Redmond, N. J. Shaw, and I. Uhlendorf, J. Phys. Chem. B **101**, 10281 (1997).
[34] H. Tang, F. Levy, H. Berger, and P. E. Schmid, Phys. Rev. B **52**, 7771 (1995).
[35] J. Orenstein and M. Kastner, Phys. Rev. Lett. **46**, 1421 (1981).
[36] P. W. M. Blom and M. C. J. M. Vissenberg, Phys. Rev. Lett. **80**, 3819 (1998).
[37] S. Berleb and W. Brütting, Phys. Rev. Lett. **89**, 286601 (2002).
[38] H. Scher and E. Montroll, Phys. Rev. B **12**, 2455 (1975).
[39] S. Nakade, W. Kubo, Y. Saito, T. Kanzaki, T. Kitamura, Y. Wada, and S. Yanagida, J. Phys. Chem. B **107**, 14244 (2003).
[40] T. Dittrich, J. Weidmann, F. Koch, I. Uhlendorf, and I. Lauermann, Appl. Phys. Lett. **75**, 3980 (1999).
[41] T. Dittrich, J. Weidmann, V. Y. Timoshenko, A. A. Petrov, F. Koch, M. G. Lisachenko, and E. Lebedev, Mater. Sci. Eng., B **69–70**, 489 (2000).
[42] T. Dittrich, E. A. Lebedev, and J. Weidmann, Phys. Status Solidi A **165**, R5 (1998).
[43] H. G. Agrell, G. Boschloo, and A. Hagfeldt, J. Phys. Chem. B **108**, 12388 (2004).
[44] F. Meng and R. Cui, J. Appl. Phys. **90**, 3387 (2001).
[45] A. Iribarren, R. Castro-Rodríguez, V. Sosa, and J. L. Pena, Phys. Rev. B **60**, 4758 (1999).
[46] J. A. Anta, J. Nelson, and N. Quirke, Phys. Rev. B **65**, 125324 (2002).
[47] L. Forro, O. Chauvet, A. Emin, L. Zuppiroli, H. Berger, and F. Levy, J. Appl. Phys. **75**, 633 (1994).
[48] J. E. Kroeze, T. J. Savenije, and J. M. Warman, J. Am. Chem. Soc. **126**, 7608 (2004).